FUDMA Journal of Sciences (FJS)
ISSN: 2616-1370
Vol. 2 No. 1, April, 2018, pp 116-129

MICRO-CLIMATIC PATTERNS OF LAND DEGRADATION/DESERTIFICATION STATUS IN A PART OF NORTH-EASTERN SUDANO-SAHELIAN ZONE OF NIGERIA

Ndabula, C[1]., Jidauna, G.G[1]., Oyatayo, K[2]., and Ati, O.F.[1]

[1]Department of Geography and Regional Planning, Federal University Dutsin-Ma, Katsina State
[2]Department of Geography, Kwararafa University Wukari, Taraba State, Nigeria
Corresponding author: cndabula@fudutsinma.edu.ng

ABSTRACT
This study aimed at assessing and mapping patterns of Micro-Climatic Sensitivity Areas (MCSA) to depict the spatio-temporal patterns of desertification status This was achieved based on the evaluation and mapping of a micro-climatic sensitivity index (MCSI) and sensitivity areas (MCSA) respectively. This was derived from three micro-climatic indices Aridity Index (AI), Land Surface Albedo Index (LSA), and Land Surface Temperature Index (LST) using the MEDALUS approach. These indicators mapped using acceptable algorithm on relevant landsat satellite data bands of (1987, 2000, and 2015) and rainfall data for the corresponding years of the satellite images. Spatio-temporal patterns of desertification status (extent, rate and intensity) was determined based on the extents of sensitivity classes using landscape change structural indices; Dynamic Rate of Change (K_i), Change Intensity (L_i) indices, while Annual Rate was estimated using logarithmic approach. Results showed that of the 30373 km^2 total extent of study area, the distribution of mean extents of various micro-climatic sensitivity areas (MCSAs) as follows; Very High, 4348 km^2 (14.32%), High, 6035 km^2 (19.87%), Moderate, 8247 km^2 (27.15%), Low, 5975 km^2 (19.67%) and Very Low, 5770 km^2 (18.99%). Annual rate of expansion which were generally observed to be low were as follows; VH, 1.139 km^2, H, 0.949 km^2 and M, 0.917 km^2 and decline; Low, 1.00 km^2, VL, 1.16 km^2. Intensification of desertification for the whole period were generally very low as follows; VH, 0.01%, H, 0.03% and M, 0.008%, while rejuvenation was also characteristically very slow as follows; L. 0.013%, VL, 0.035%. Dynamic rates of change for the period were also very slow as follows; VH, 0.235%, H, 0.635%, M, 0.135%, L, 0.187% and 0.812%. This micro-climatic approach is preponderant for eco-remediation approach in combating land degradation and desertification.

Keywords: Desertification, Micro-climatic, Eco-remediation, Sensitivity, Aridity, Albedo.

INTRODUCTION

The most authoritative definition of *desertification* remains that of the Convention to Combat Desertification: "land degradation in arid, semi-arid and dry sub-humid areas resulting from various factors, including climatic variations and human activities" (UNEP 1994, UNCCD, 1995). Land degradation is, however, difficult to grasp in its totality. Land degradation is a composite term; it has no single readily-identifiable feature, but instead describes how one or more of the land resources (soil, water, vegetation, rocks, air, climate, relief) has changed for the worse. In the current study, the reference to present-day climate-induced desertification is related either to climate variability and climate change. Recent studies indicate that triggering factors of land degradation such as climatic variability, climate change have resulted in drier conditions in arid and semi-arid regions (Held et al., 2005; Burke et al., 2006; Seager et al., 2007). Increase in aridity can result in a wide range of changes on the land surface characteristics including diminution of vegetation cover, increase bare surfaces, changes in thermal and reflectivity of the land surface. All these changes in land surface characteristics in feedback mechanism may affect regional climatic, micro-climatic, hydro-climatic and eco-geomorphic systems and consequently desertification.

Desert eco-geomorphic systems are typically fragile and even small perturbations can have long-lasting impacts on the distribution of vegetation and on functionality of the landscape (Schlesinger et al., 1990; Okin et al., 2004, Ndabula, 2015). Vegetation change may have positive feedbacks to climate that accelerate change (Scheffer et al., 2005; Beatley, 1980).

Severe climatic conditions such as persistent droughts that affected sub-saharan Africa since the late 1960s combined with poor land management and unsustainable use of marginal resources exacerbate land degradation and desertification. Anthropogenic pressures such as overgrazing, over-cultivation, urbanization on the semi-arid land which has been described as ecologically marginal (Chen et al., 2015) cause adverse changes in the hydrologic and geomorphic processes thereby extending and intensifying desertification.

It can also be said that climatic variation is both cause and effect of desertification. Just as climatic variations have been acclaimed as underlying (indirect) drivers or triggering factors of land degradation and desertification, so also do they remain the underlying and usually not easily observable effects or impacts and imprints of land degradation and desertification (Ndabula, 2015). Climatic factors, mainly associated with a decrease in rainfall (reduced by as much as 1.5% annually over the last quarter of the 20th century in southern Africa), are prominent underlying driving forces of desertification (86%). They operate either indirectly, through changes in land use resulting from variation in rainfall or directly, affecting land cover in the form of prolonged droughts (such as the 1973–1977 period in semiarid parts of the Sub-saharan and west Africa, Although more than one-third of the studies mention climatic influences but fail to explicitly describe them, the most

widespread mode of causation is reported to be climatic conditions operating concomitantly or synergistically with socioeconomic driving forces, such as technological changes.Meteorological conditions are also part of feedback loops related to desertification.

Micrometeorological conditions of land surface like aridity, temperature, wind and albedo have been used to characterize desertification. These changes of land surface conditions make the spectral characteristics of desertification land vary greatly to different degrees, which could be captured by satellite sensors and this might be fundamental for the analysis of desertification by means of the indices derived from satellite images (Pinet et al, 2006). The Climate quality is calculated from indicators that influence soil and water availability to plants such as solar radiation, temperature, amount of rainfall, evaporation, albedo and aridity index.

Land surface temperature is sensitive to vegetation and soil moisture; hence it can be used to detect land use/land cover changes especially due to land degradation and desertification etc. Land surface temperature (LST), controlled by the surface energy balance, atmospheric state, thermal properties of the surface, and subsurface mediums, is an important factor controlling most physical, chemical, and biological processes of the Earth (Becker and Li, 1990). Similarly changes in LST is an indicator of changes in biogeochemical processes which can be used to assess land degradation and desertification processes. Land surface temperature can provide important information about the surface physical properties and climate which plays a role in many environmental processes (Dousset & Gourmelon 2003; Weng, Lu & Schubring 2004).

These changes of land surface conditions make the spectral characteristics of desertification land vary greatly to different degrees, which can be captured by satellite sensors. This may be fundamental for quantitatively assessing desertification by means of the indices derived from satellite images, because the accuracy of soil properties acquired from satellite images is very variable.

Spatialisation of land surface energy fluxes and evapo-transpiration from remote detection data in visible, near infrared and thermal infrared regions of the electromagnetic spectrum has been at the centre of many meteorological approaches during the last past years (Arouna et al., 2013). Remote sensing data provide an efficient cost effective means to assess biophysical indicators of land degradation and desertification, providing that essential ecosystem properties can be monitored. An increased use of satellite data to monitor the albedo of arid lands has arisen from the dual importance of albedo as a potential indicator of arid land degradation and as a physical parameter with possible impacts on climate. Albedo may serve as an indicator of degradation because removal of vegetative cover exposes more of the soil background, which is generally highly reflective. Albedo and other satellite measures of overall reflectivity thus tend to increase when overgrazing or prolonged drought lead to decreases in vegetative cover, and reflectivity decreases with recovery (Musick, 1986). Some studies found that land surface broadband albedo is a critical variable affecting the earth's climate. In semiarid regions, an increase in albedo leads to a loss of radiation energy absorbed at the surface, and convective overturning is reduced. As a result, precipitation decreases. Evaporation may also decrease, further inhibiting precipitation (Liang, 2000). Land surface albedo is an important indicator that determines energy budget and the change of micrometeorological conditions like temperature, aridity/humidity etc. of land affected by desertification (Pinet et al, 2006). Harazono's observation research (Li et al., 2000) show that the land surface appears the first sign of sandy desertification with a corresponding threshold of 30 per cent of surface albedo, and indicated that the surface albedo have intrinsic relationship with the land desertification dynamic. Surface albedo is the most important physical parameters used to characterize underlying surface radiation characteristics. It is affected by the change of solar altitude angles, meteorological conditions, surface coverage type, soil moisture and terrain, etc (Fang et al., 2001).

The Plan action To Combat Desertification as agreed in the (UNCOD, 1977) was clear on its stand that development and adoption of sustainable actions to combat desertification or land management practices especially in desert prone areas requires more specific and accurate understanding of the role of climatic factors in land degradation or desertification. The Convention calls on the affected country parties to address the underlying causes of desertification and it is timely that more efforts be devoted to better understand the role of climatic factors. It is on this account that a study like seek to explore more details of understanding specific roles of climatic indicators of causes and effects of desertification. There is the need to adopt an approach or methodology that explain the spatio-temporal patterns of these micro-climatic indicators to better estimate the status of desertification a crucial aspect that is vital for dealing all contentious issues on the subject

It is a well established fact from literature that climatic variations (drought/aridity, albedo changes etc) are both predisposing and triggering factors or causes of desertification (Santini et al, 2003). Also, Symeonakis and Drake (2004) have summarized the effects of desertification on vegetation and finally on soil. However, the general understanding of land surface complex biogeophysical and biogeochemical feedbacks under desertification generate more specific micro-climatic among pedo-geomorphic, eco-hydrological effects. Hencey, it has been widely reported that desertification or land degradation is accompanied by changes in land surface characteristics such as changes in albedo, land surface temperature, aridity and several anomalies in land surface radiation fluxes. Monitoring the spatio-temporal patterns of these land surface micro-climatic variables can be viewed as desertification status indicators and thus provide more understanding to eco-remediation approach in combating desertification hazard.

STUDY AREA

The Sudano-Sahelian ecological zone in Nigeria has its southern boundary crossing latitude 12°N on the western frontier to latitude 10°N 30' on the eastern frontier, extending to latitude 14°N as the northernmost boundary (Kowal and Knabe, 1972; Mortimore, 1989).

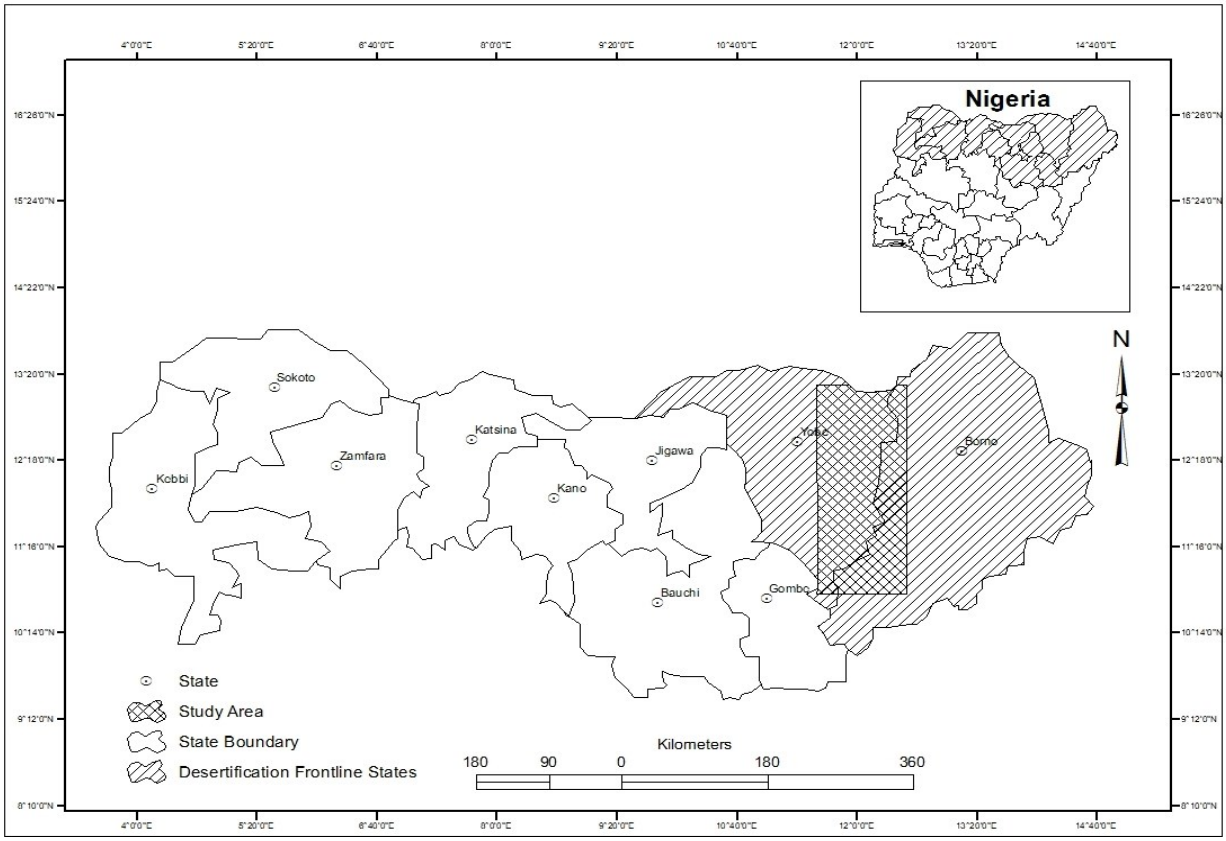

Fig 1: Map of Desertification Frontline States showing Study Area
Source: Ndabula, 2015

The Physical Setting

The climate is semi-arid with wide seasonal and diurnal temperatures. A long dry season is followed by a single short wet season. The hottest months are March to May. The cold and dry dust-laden north easterly Harmattan winds prevail from November to March, with significant diurnal temperature fluctuations and extremes of temperature (Rayar, 1987). Rainfall is seasonal with a wet season occurring from July to September; with mean annual rainfall varying between 1000-500 mm from south to north. Rainfall is highly variable in space and time with high intensities (Ati, 2006). Recent years have seen decreasing annual rainfall totals (Cater and Alhassan, 1998) and dry spell is becoming a frequent problem in the area (Oladipo, 1994).

The soils of Borno-Yobe vary in color, texture, structure, physic-chemical and other essential characteristics. Fig3.1.2.4 reveals the distributin of soil. Vertisols (dark heavy clay soils (firkin)) dominate the flat plains close to Lake Chad and most parts of wetlands and floodplains. Regosols found mainly in the sand dunes are shallow with weakly developed profiles.

The vegetation is dominantly of sudan and sahel savanna and is characterized by sparse shrubs, grasses and woody trees such as Gum Arabic (*Acacia albida* and *Acacia nilotica*),Guinea grass (*Pennisetum maximum*), Buffel grass (*Cenkhras ciharis*), star grass (*Cynodom nlemficensis*),Elephant Grass (*Pennisetun purpureum*), Gamba grass (*Andropogon gayanus*), Baobab tree (Andosonia digitata), Shea butter tree or kadanya (*Butyrospernun parkii*), Neem tree (*Azandrata indica*), Silk cotton, Dum palm etc. Vegetation covers is sparse on the grass grows in individual tufts leaving bare surfaces in between.

MATERIALS AND METHODS

In order to assess and map the spatio-temporal patterns of micro-climatic sensitivity areas to depict desertification status (ie extent, rate and intensity). The approach to achieve this was based on the evaluation of a micro-climatic sensitivity index (MCSI) derived from three micro-climatic indices Aridity Index (AI), Land Surface Albedo Index (LSA), and Land Surface Temperature Index (LST) using the MEDALUS approach. These variables which represent cause-effect relationship and indicators of desertification were evaluated and mapped using acceptable algorithm on relevant satellite data bands of (1987, 2000, and 2015) and rainfall data for the corresponding years of the satellite images. The various single and combined output micro-climatic indices maps were classified into five (5) micro-climatic sensitivity areas based on natural jenks method. Spatio-temporal patterns of desertification status (extent, rate and intensity) was determined based on the extents of sensitivity classes using landscape change structural indices; dynamic rate of change (K_i), change intensity (L_i) indices and annual rate using logarithmic approach (Ndabula et al , 2013 and Ndabula, 2015).

Evaluation and mapping of aridity index (AI) and sensitivity index (ASI)

Aridity Index (AI) was achieved through GIS interpolation of raster surfaces from climatic data (rainfall and temperature) to

generate the multi-temporal rain-surface and PET-surface sets of 1987, 2000 and 2015.

AI = P/PET ……(1)

Where

P = Annual Precipitation (for a given year, 1987, 2000, and 2015 respectively)

PET = Annual Potential Evapotranspiration (for a given year, 1987, 2000, and 2015 respectively)

$PET = P/(0.9 + (P/L)^2)^{1/2}$ (Jones, 1997)……(2)

Where

$L = 300 + 25T + 0.05T^3$.....(3) and where T = mean annual temperature.

Both P and PET were calculated as point values then interpolated using kriging method to generate raster rain surface (P) and PET respectively in ArcGIS. Finally, an aridity raster map was computed using ArcGIS.

Multi-temporal sets of the AI were then generated

Then the ASI was generated from the geometric mean of the three multi-temporal mapsets AI_87, AI_2000 and AI_2015.

$ASI= \sum(AI\_87 + AI\_2000 + AI\_2015)^{1/3}$

Evaluation and mapping of land surface temperature (LST) and sensitivity index (LSTSI)

This was achieved using thermal bands of landsat multi-temporal images (1987, 2000, 2015). LST is a good indicator of changes on the earth surface especially due to land degradation or desertification.

Conversion to At-Satellite Brightness Temperature

TIRS band data can be converted from spectral radiance to brightness temperature using the thermal constants provided in the metadata file:

$$T = \frac{K_2}{ln(\frac{K_1}{L_\lambda}+1)} \quad \text{……(11)}$$

Where:

T = At-satellite brightness temperature (K) (for the 1987, 2000, 2015 respectively)

L_λ = TOA spectral radiance (Watts/(m2 * srad * μm)

where,

L_λ = $(Lmax_\lambda - Lmin_\lambda)/(Qcalmax-Qcalmin))*(Qcal-Qcalmin) + Lmin_\lambda$

K_1 = Band-specific thermal conversion constant from the metadata

K_2 = Band-specific thermal conversion constant from the metadata

For L5, TM: K1 = 607.76 (W/m^2sr um); K2 = 1260.56K

For L7, ETM^+: K1 = 666.09 C); K2 = 1282.71K

For L8, OLI/TIR: K1 = 774.89 (W/m^2srum)

K2 = 1321.08K

The LSTSI was generated from the geometric mean of the three multi-temporal mapsets of LST.

$LSTSI= \sum(LST\_87 + LST\_2000+ LST\_2013)^{1/3}$

Evaluation and mapping of land surface albedo (LSA) and sensitivity index (LSASI)

In this study the approach adopted by Guo *et al* (2010) who determined broadband albedo by the combination of narrowband albedo to assess the micrometeorological conditions of land surface. Broadband albedo was then calculated according to its relationship with each narrowband. The broadband calculation for Landsat.TM and ETM and Landsat.OLI/TIR used the equations

Broad band albedo (TM/ETM^+ i.e 1987 and 2000) = $0.356\alpha_1 + 0.130\alpha_3 + 0.373\alpha_4 + 0.085\alpha_5 + 0.072\alpha_7 – 0.0018$……(4)

Broad band albedo (OLI/TIR i.e 2015) = $0.356\alpha_2 + 0.130\alpha_4 + 0.373\alpha_5 + 0.085\alpha_6 + 0.072\alpha_7 – 0.0018$…….(5)

Where α1……. α7 are the narrow bands (P_λ) for respective bands which were previously calculated and mapped using the formula

$P_\lambda = \pi \times L_\lambda \times d^2/ESUN_\lambda \times COS(\Theta)_s$……(6)

and OLI/TIR

$$\rho\lambda = \frac{\rho\lambda'}{\cos(\theta_{SZ})}$$

Where,

$\rho\lambda' = M_\rho Q_{cal} + A_\rho$

LSASI was then generated from the geometric mean of the three multi-temporal mapsets of LSA

$LSASI= \sum LSA\_87 + LSA\_2000 + LSA\_2015)^{1/3}$

To assess the spatio-temporal pattern of LSA and LSASI

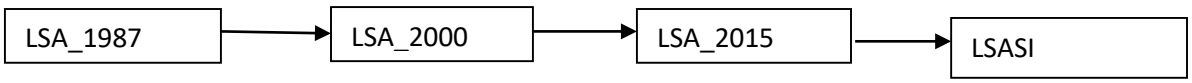

The multi-temporal sets of LSA (1987, 2000 and 2015) are generated from corresponding temporal landsat images and LSASI from the sensitivity analysis of the geometric mean of the three sets of LSA that have been generated in raster map format

$LSASI= \sum LSA\_87 + LSA\_2000 + LSA\_2015)^{1/3}$

All the LSA and LSASI raster maps were classified using natural breaks (jenks) to reveal spatio-temporal patterns based on hierarchical organization in the landscape. The extent, rate and intensity of change were computed.

To assess the spatio-temporal pattern of LST and LSTSI

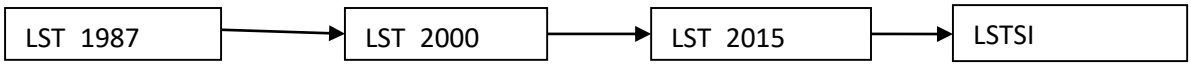

The multi-temporal sets of LST (1987, 2000 and 2013) and LSTSI are generated from corresponding temporal landsat images and LSTSI from the sensitivity analysis of the geometric mean of the three sets of LST that have been generated in raster map format

$LSTSI = \sum(LST\_87 + LST\_2000 + LST\_2015)^{1/3}$

All the LST and LSTSI raster maps were classified using natural breaks (jenks) to reveal spatio-temporal patterns based on hierarchical organization in the landscape. The spatio-temporal patterns of extent, rate and intensity of change were estimated.

To Assess the Spatio-temporal Patterns of Micro-climatic Sensitivity Index (MCSI)

This is achieved based on analysis the three sets of multi-temporal micro-climatic indices and their respective sensitivity indices (AI, LSA, LST and ASI, LSASI, LSTSI) maps and generation of micro-climatic sensitivity index (MCSI) map using the MEDALUS model approach. The MCSI map is then reclassified into five (5) micro-climatic sensitivity areas

Flow Chart to Assess the Spatio-temporal Patterns of Aggregated Micro-climatic Sensitivity Index

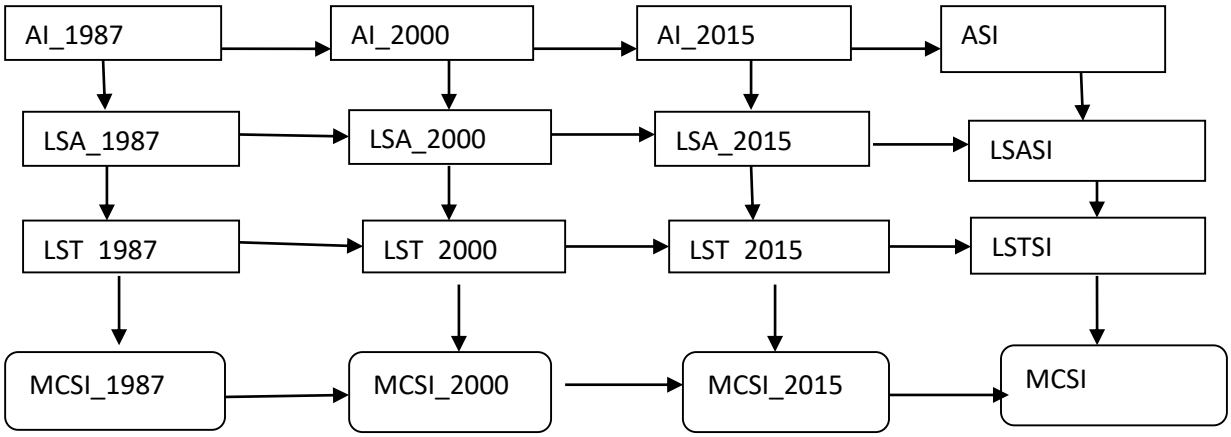

The horizontal dimensional analysis algorithm:

$ASI = \sum(AI\_87 + AI\_2000 + AI\_2015)^{1/3}$

$LSASI = \sum LSA\_87 + LSA\_2000 + LSA\_2015)^{1/3}$

$LSTSI = \sum(LST\_87 + LST\_2000 + LST\_2015)^{1/3}$

$MCSI = \sum(ASI + LSASI + LSTSI)^{1/3}$

ASI = Aridity Index
LSASI = Land Surface Albedo
LSTSI = Land Surface Temperature
Mapped into sensitivity areas using jenk's method
ASA = Aridity Sensitivity Areas
LSASA = Land Surface Albedo Sensitivity Areas
LSTSA = Land Surface Temperature Sensitivity Areas

The vertical dimensional analysis algorithm:

$MCSI\_87 = \sum(AI\_87 + LSA\_87 + LST\_87)^{1/3}$

$MCSI\_2000 = \sum(AI\_2000 + LSA\_2000 + LST\_2000)^{1/3}$

$MCSI\_2013 = \sum (AI\_2015 + LSA\_2015 + LST\_2015)^{1/3}$

$MCSI = \sum(MCSI\_87 + MCSI\_2000 + MCSI\_2015)^{1/3}$

Where;
MCSI = Micro-climatic Sensitivity Index
MCSA = Micro_Climatic Sensitivity Areas

RESULTS AND DISCUSSIONS

A general rule of the thumb applied for the interpretation of is: Increase or expansion in the Very High, High and Moderate represents land degradation or desertification while expansion in the Low and Very Low sensitivity areas represents reversibility of desertification effects.

The results and discussions for the specific micro-climatic indicators are presented as follows;

Aridity Sensitivity Areas (ASA)

From Table 1a and Fig 1a: the result shows that there is a general northward shift in the aridity sensitivity boundaries with increasing trend in extents in favour of the Moderate, High and

Very High aridity sensitivity areas which account for about 74% of the study area with a corresponding decline the extents in the Very low and Low sensitivity areas. The Spatio-temporal patterns of Aridity sensitivity areas status showed that the largest mean extent for the period (1987-2015) of 9132km^2 is classified under the high aridity sensitivity followed by the very high aridity sensitivity area with mean extent of 8116 km^2.and moderate 5265 km^2. These three classes have shown respective expansion in extent as follows; 1915 km^2, 1469 km^2 and 170 km^2. These expansions represent respective annual expansion rates of 1.26 km^2, 1.22 km^2 and 0.86 km^2 and intensification of 0.063%, 0.048% and 0.006%. In the southernmost parts the low aridity sensitivity areas has mean extent of 4012km^2 and the least very low aridity sensitivity areas 3486km^2. The highest annual rate of change of 1.28km^2 was observed in the very low sensitivity areas, followed closely by high 1.26km^2, very high 1.22km^2 and the least moderate class 0.86km^2. Similar patterns were also observed for change intensity. The highest being is 7.0% in the very low class, followed by 6.3% and 4.8% in the high and very high sensitivity areas respectively. The patterns of dynamic rate of change differ slightly where the highest dynamic rate of 1.46% was recorded in the very low aridity sensitivity class, followed by High 1.02%, Low 1.0% very high 0.85% and the least moderate 0.12%

Land Surface Albedo Sensitivity Areas (LSASA)

From Table 1b and Fig 1b: The Spatio-temporal patterns of land surface albedo sensitivity areas status showed that the largest extent of 7398 km2 was registered in the high sensitivity areas, followed by moderate, 7113 km^2, low, 6932 km^2, very high, 4742 km^2 and the least 4187 km^2 in the very low sensitivity areas. However, expansion was only recorded in the High and Moderate sensitivity areas representing 1720 km^2 and 3260 km^2 respectively. This put annual expansion in these two classes at 1.24 km^2 and 1.35 km^2 and change intensity of 0.057 and 0.107% respectively. This expansion in high and moderate albedo sensitivity areas be associated to the decline in vegetation cover and sandification observed in these areas based on NDVI and GSI analysis reported by Ndabula (2015). Albedo and other satellite measures of overall reflectivity thus tend to increase when overgrazing or prolonged drought lead to decreases in vegetative cover, and reflectivity decreases with recovery (Musick, 1986). Land surface albedo is an important indicator that determines energy budget and the change of micrometeorological conditions like temperature, aridity/humidity etc. of land affected by desertification (Pinet et al, 2006; Li et al., 2000)

Land Surface Temperature Sensitivity Areas (LSTSA)

From Table 1c and Fig 1c: the mean extent of the various land surface temperature sensitivity areas as follows; Very High; 5024 km^2, High, 6328 km^2 Moderate 4936 km^2, low, 3111 km^2 and Very Low, 10, 075 km^2 respectively. With the exception of the High class which has declined in extent by 4464 km^2 all others have recorded expansion as follows; High (410 km^2), moderate (231 km^2), Low (3591 km^2) and Very Low (227 km^2). These changes when evaluated to represent annual rate, change intensity and dynamic rate of desertification gave a wide range of variation among the classes. The highest annual rate of desertification of 1.40 km^2 was observed in the high sensitivity areas, followed closely by the low sensitivity areas with 1,37 km^2 and the least 0.91 km^2 in the both the moderate and very low sensitivity areas. Change intensity rates for the period also varied. The highest change intensity of 14.07% was recorded in the high sensitivity areas , followed by 11.82% in the low sensitivity class, and the least 1.35% in the very high sensitivity areas. The dynamic rate of change for the period were characteristically low, except for the low sensitivity areas that reflected an exceptionally high dynamic rate of 65.46% which is believed might be due to image discrepancies or interpretation related problem.

Micro-Climatic Sensitivity Areas (MCSA) based on the analysis and mapping of MCSI

From Table 1d and Fig 1d; The current spatial distribution of micro-climatic sensitivity areas that the greater part of the semi-arid area of 30373 km^2 under study lies in the moderate micro-climatic sensitivity area with an extent of 8247km2 or 27%), followed by the high sensitivity areas of about 6035 km^{2}or 19.86%, moderate of 5975 km^2 or 19.67%, very low sensitivity of 5770km2 or 19.00% and the least being the very high sensitivity with an extent of about 4348 km^2 or 14.32%. The variation in the annual rates of change, change intensity and dynamic rates for the period were as follows; the low micro-climatic sensitivity areas has lost a total 1050 km^2 to due conversion towards higher sensitivity areas making it to record the highest annual rate of change of 1.16 km^2, change intensity for the period under review of 3.50% and dynamic rate for the period of 0.812%. The high sensitivity areas ranked second with a total change in extent of 916 km^2 over the period to record an annual rate of change of 1.139 km^2, change intensity and dynamic rate for the period of 3.02% and 0.64% respectively. The low sensitivity areas which recorded a net loss in its extent of about 400 km^2 likely due to the corresponding conversion to higher sensitivity areas was represented with an annual rate of change of 1.00 km^2, change intensity and dynamic rate for the period of 1.3% and 0.187%. The very high sensitivity areas recorded a net areal expansion of 293 km^2 for the period, which represented an annual rate of change of 0.95km2, change intensity of 1.00% and 0.238% dynamic rate for the period. The least with a net change in extent is the moderate sensitivity areas which represented an annual rate of change of 0.917km2, change intensity and dynamic rate for the period of 0.8% and 0.135% respectively. The general micro-climatic that there has been a gradual but persistent shifting pattern from lower micro-climatic sensitivity areas towards higher sensitivity areas. The various sensitivity areas also indicated variation in the annual rates of change and change intensity and dynamic rates for the period.

CONCLUSION AND RECOMMENDATIONS

The approach adopted in this study of evaluating, mapping and analysis micro-climatic sensitivity areas as a basis for determining the status ie extent, rate and intensity of desertification provided a new and more reliable estimates of desertification status. The selection of specific micro-climatic indicators; Aridity, land surface Albedo and Land surface Temperature in agreement of the assertion of Warren (2002) that desertification or land degradation is contextual especially with respect to causal indices. The result of the three (3) indicators although reveals slight similarities but different patterns and hence status of desertification in the study area.

The results as revealed in this study established that that desertification is mostly observed to be persistent and

progressive in the most climatically sensitive areas especially the Moderate, High and Very High Micro-climatic Sensitivity Areas as classified in this study. In the southern part of the study area which fall under the Low and Very Low sensitivity areas it is generally observed that factors are not persistent, rather the area is showing remarkable recoverability or reversibility from desertification.

This micro-meteorological approach in this study contributes to the better interpretation of such dynamic and a best comprehension of the biophysical mechanisms intervening in soil/plant's system. This is vital for eco-remediation approach as a part of combating desertification and putting plan of management and adequate conservation of the semi-arid landscape.

Table1a: Spatio-temporal Patterns of Aridity Sensitivity Areas Status in the Semi-arid Zone of Nigeria (Based on Analysis of ASI)

Class of Sensitivity Area (SA)	Extent of i^{th} class of SA in km^2 1987 (Uai)	Extent of i^{th} class of SA in Km^2 2000	Extent of ith class of SA in Km^2:2013 (U_{bi})	Mean Extent of ith class of SA in Km2 based on ASI (Ubi1)	Change in extent of i^{th} SA in Km^2 for study period (U_{bi}-U_{ai})	Annual Rate of change of i^{th} SA in Km^2 (Li)	Change intensity index for i^{th} class of SA for the study period (T_i)	Dynamic index for i^{th} class of SA in % for the study period (K_i)	proportion of contribution by i^{th} class of SA for the study period (A_i)
1-VeryHigh	6647	7038	6598	8116	1469	1.22	0.048	0.850	0.207
2- High	7217	7066	6610	9132	1915	1.26	0.063	1.021	0.269
3- Moderate	5455	5677	6579	5625	170	0.86	0.006	0.120	0.024
4- Low	5439	5520	5701	4012	-1427	-1.21	-0.047	-1.009	-0.201
5- Very low	5613	5071	4882	3486	-2127	-1.28	-0.070	-1.457	-0.299
Total Area	**30372**	**30372**	**30373**	**30372**	**∑ = 7108**				

Table1b: Spatio-temporal Patterns of Land Surface Albedo Sensitivity Areas Status in the Semi-arid Zone of Nigeria (Based on LSASI)

Class of Sensitivity Area (SA)	Extent of i^{th} class of SA in km^2 1987 (Uai)	Extent of i^{th} class of SA in Km^2 2000	Extent of ith class of SA in Km^2:2013 (U_{bi})	Extent of ith class of SA in Km2 based on LSASI (Ubi1)	Change in extent of i^{th} SA in Km^2 for study period (U_{bi}-U_{ai})	Annual Rate of change of i^{th} SA in Km^2 (Li)	Change intensity index for i^{th} class of SA for the study period (T_i)	Dynamic index for i^{th} class of SA in % for the study period (K_i)	proportion of contribution by i^{th} class of SA for the study period (A_i)
1-VeryHigh	4317	3459	4007	4742	-310	0.96	-0.010	-0.276	-0.031
2- High	7018	6384	8738	7398	1720	1.24	0.057	0.943	0.173
3- Moderate	7204	5149	10464	7113	3260	1.35	0.107	1.740	0.327
4- Low	7018	14960	6636	6932	-382	0.99	-0.013	-0.209	-0.038
5- Very low	4816	420	527	4187	-4289	1.40	-0.141	-3.425	-0.431
Total Area	**3072**	**3072**	**3072**	**3073**	**∑ = 9961**				

Source: Ndabula, 2015

Table 1c: Spatio-temporal Patterns of Land Surface Temperature Sensitivity Areas Status in the Semi-arid Zone of Nigeria (Based on LSTSI)

Class of Sensitivity Area (SA)	Extent of i^{th} class of SA in km^2 1987 (Uai)	Extent of i^{th} class of SA in Km^2 2000	Extent of ith class of SA in Km^2:2013 (U_{bi})	Extent of ith class of SA in Km2 based on LSTSI (Ubi1)	Change in extent of i^{th} SA in Km^2 for study period (U_{bi}-U_{ai})	Annual Rate of change of i^{th} SA in Km^2 (Li)	Change intensity index for i^{th} class of SA for the study period (T_i)	Dynamic index for i^{th} class of SA in % for the study period (K_i)	proportion of contribution by i^{th} class of SA for the study period (A_i)
1-VeryHigh	7048	6600	7458	5024	410	1.00	0.013	0.224	0.046
2- High	15079	1048	10615	6328	-4464	1.40	-0.147	-1.139	-0.500
3- Moderate	7522	5025	7753	4936	231	0.91	0.008	0.118	0.026
4- Low	211	6690	3802	3111	3591	1.37	0.118	65.458	0.402
5- Very low	517	2321	744	10,075	227	0.91	0.007	1.689	0.025
Total Area	**30380**	**30373**	**30373**	**30373**	**∑ = 8923**				

Source: Ndabula, 2015

Table1d: Spatio-Temporal Patterns of Micro-Climatic Sensitivity Areas Status in a part of NE semi-arid zone of Nigeria

	MCSI_1987	MCSI_2000	MCSI_2013	MCSI -1	MCSI-2	MCSI_1:2avg					
Class of Sensitivity Area (SA)	Extent of i^{th} class of SA in km^2 1987 (U_{ai})	Extent of i^{th} class of SA in Km^2 2000	Extent of i^{th} class of SA in Km^2:2013 (U_{bi})	Extent of i^{th} class Km^2	Extent of i^{th} class Km^2	i^{th} SA current extent in km^2	Change in extent of i^{th} SA in Km^2 for study period (U_{bi}-U_{ai})	Annual Rate of change of i^{th} SA in Km^2 (L_i)	Change intensity index for i^{th} class of SA for the study period (T_i)	Dynamic index for i^{th} class of SA in % for the study period (K_i)	proportion of contribution by i^{th} class of SA for the study period (A_i)
1-VeryHigh	4740	4489	5033	4183	4513	4348	293	0.949	0.010	0.238	0.101
2- High	5547	9198	6463	5982	6087	6035	916	1.139	0.030	0.635	0.316
3- Moderate	6874	11063	7116	8403	8091	8247	242	0.917	0.008	0.135	0.083
4- Low	8239	4984	7839	5908	6042	5975	-400	-1.000	-0.013	-0.187	-0.138
5- Very low	4973	640	3923	5900	5640	5770	-1050	-1.160	-0.035	-0.812	-0.362
Total Area	**30373**	**30373**	**30373**	**30373**	**30373**	**30373**	**∑ = 2901**				

Source: Ndabula, 2015

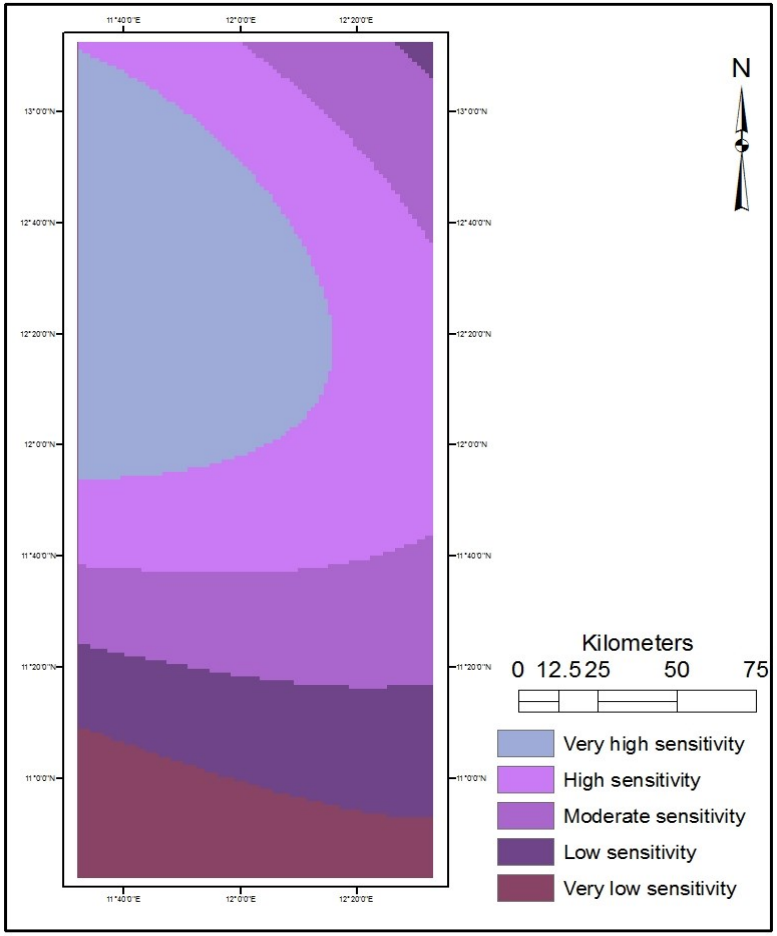

Fig 1a: Aridity Sensitivity Areas (ASA) based on ASI

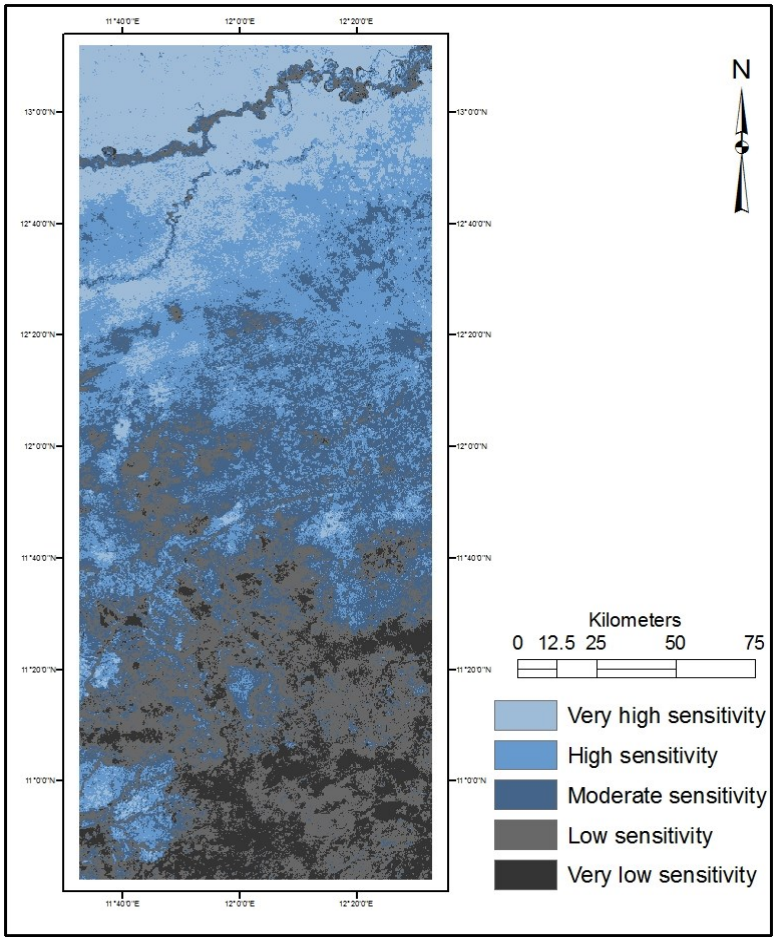

Fig1b: Land Surface Albedo Sensitivity Areas (LSASA) based on LSASI

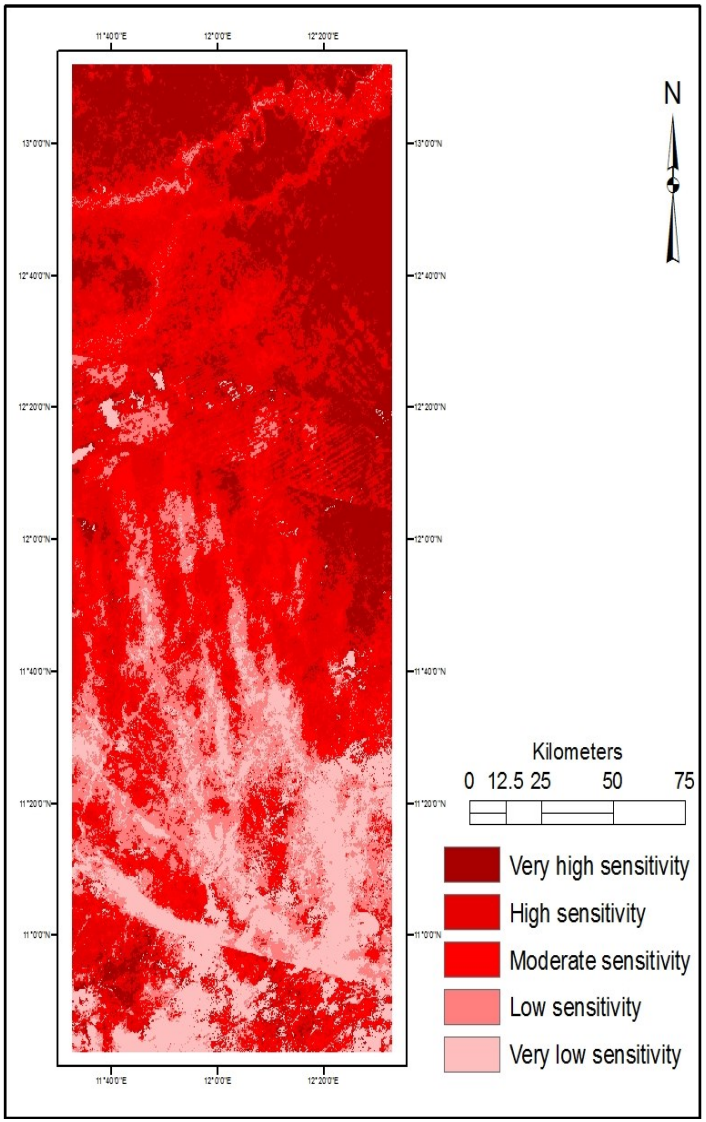

Fig 1c: Land Surface Temperature Sensitivity Areas (LSTSA) based on LSTSI

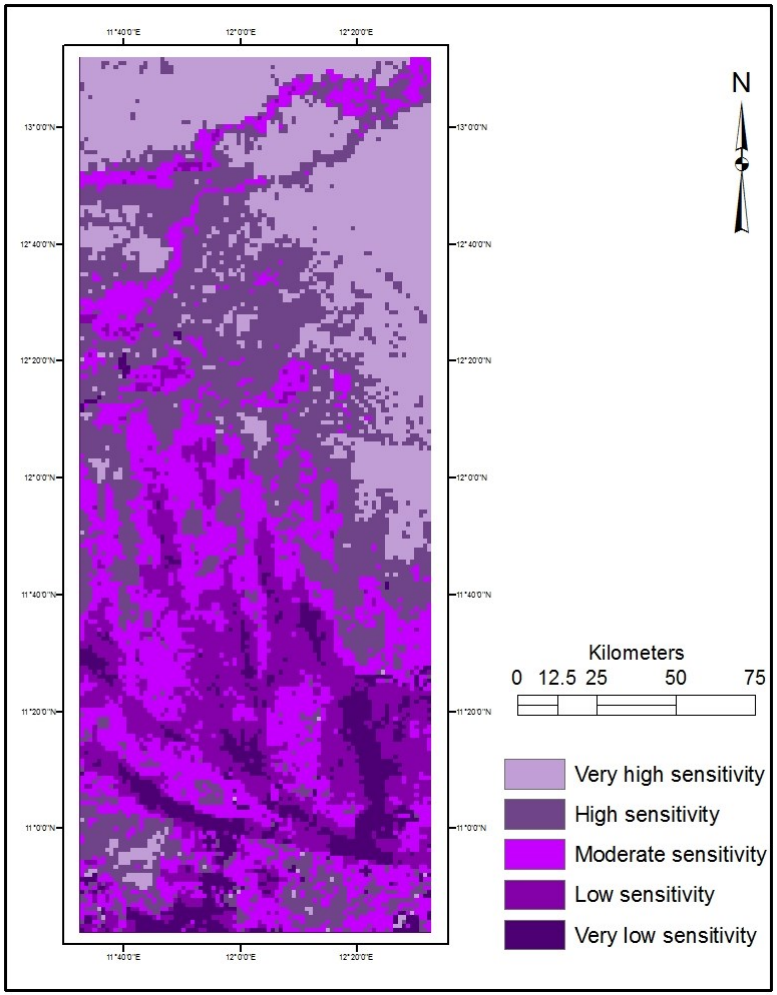

Fig 1d: Micro-Climatic Sensitivity Areas (MCSA) based on MCSI

REFERENCE

Arouna, S.H., Oumar, D and Amadou, S.M. (2013). A Spatial Analysis of Surface Energy Fluxes and Evapo-transpiration in the Northern-east of Niger W National Park. Research Journal of Environmental and Earth Science 5(3): 123-130, 2013.

Ati, O.F. (2006). Rainfall characteristics in drought prone sudano-Sahelian zone of Nigeria. Unpublished Ph.D thesis, Department of Geography Ahmadu Bello University, Zaria.

Becker, F. and Z. L. Li. (1990). Towards a local split window method over land surfaces. *Int. J. Remote Sensing*, 11:3.

Chen,S., Su, H., tian, J., and Yu, J. (2015). Spatial-Temporal processes of desertification and oasification in the middle reaches of the Heihi River based on remote sensing. Remote Sensing Journal 33(2): 347-353.

Dousset, B. & Gourmelon, F. (2003). Satellite multi-sensor data analysis of urban surface temperatures and landcover, ISPRS Journal of Photogrammetry and Remote Sensing. 58, (1-2), 43-54.

Fang, J. Y., S. L. Piao, Z. Y. Tang, C. H. Peng, *and* W. Ji *(*2001*),* Interannual variability in net primary production and precipitation*,* Science*,* 293*,* 1723.

M. Guo, M., Liu, Y., Wang, X.F., Matsuoka, N and Tani, H. (2010)Analysis of desertification and wood land distribution: A case study on the Balinyou Banner of Inner Mongolia, China

Kowal, J.N., and Knabe, D. (1972). An agroclimatological atlas of northern states of Nigeria. Ahmadu Bello University Press, Zaria.

Mortimore, M (1989). Adapting to drought: farmers, famines, and desertification in west Africa. Cambridge University Press, New york, USA.

Musick H.B. (1986). Temporal change of Landsat MSS albedo estimates in arid rangeland. Remote Sens. Envrion. 20:107–120.

Ndabula, C., Averik P. D., Jidauna G.G., Abaje I., Oyatayo T. K., E. O Iguisi (2013) . Analysis of the Spatio-Temporal Dynamics of Landuse/ Landcover Stuctures in the Kaduna Innercore City Region, Nigeria, *American Journal of Environmental Protection, (USA). Vol. 1, No. 4, 112-119.* http://pubs.sciepub.com/env/1/4/7.

Ndabula, C. (2015). Assessment of the spatio-temporal patterns of biosphysical indicators of desertification status in the semi-arid zone of Nigeria. Unpublished PhD. Thesis in the Department of Geography Ahmadu Bello University, Zaria.

Okin, G.S., Mahowald, N., Chadwick, O.A., and Artaxo, P. (2004). Impact of desert dust on the biogeochemistry of phosphorus in terrestrial ecosystems. *Global Biogeochem. Cy. 18,* Art. No. GB2005.

Oladipo, E.O. (1994). Some aspects of the spatial characteristics of drought in northern Nigeria. Natural Hazards 8: 171-188.

Pinet, P.C.; Kaufmann, Cill, .; H J**.** (2006) Imaging spectroscopy of changing Earth's surface: a major step toward the quantitative monitoring of land degradation and desertification. C. R. Geosci. 338, 1042-1048.

Rayar, A.J. (1987). Studies on some physico-chemical parameters of soils of Borno state. Annals of University of Maiduguri, 4: 283-291.

Scheffer, M., Holmgren, M., Brovkin, V., and Claussen, M. (2005). Synergy between small- and largescale feedbacks of vegetation on the water cycle. *Glob. Change Biol. 11*, pp. 1003-1012. Beatley, J.C. (1980). Fluctuations and Stability in Climax Shrub and Woodland Vegetation of the

Schlesinger, W.H., Reynolds, J.F., Cunningham, G.L., Huenneke, L.F., Jarrell, W.M., Virginia, R.A., and Whitford, W.G. (1990). Biological Feedbacks in Global Desertification. *Scence 247*, pp.1043-1048.

UNCCD (United Nations Convention to Combat Desertification) (1995). Elaboration of an International Convention to Combat Desertification in Countries Experiencing Serious Drought and/desertification. Particularly in Africa. U.N DocA/AC241/27,33 I.L.M. p1328 http://www.unccd.int/.USGS, 2001. Landsat 7 Science Data User's Handbook.

UNCOD, (1977). United Nations Conference on Desertification 29th Aug-9 Sept 1977, Round-up plan of action and resolutions. UNCOD-UNEP, New York, EUA, 43p.

[UNEP] United Nations Environment Programme 1994. United Nations Convention to Combat Desertification. Nairobi (Kenya): UNEP.

Weng, Q., Lu, D. & Schubring, J., 2004. Estimation of land surface temperature-vegetation abundance relationship for urban heat island studies, Remote Sensing of Environment, 89(4), 467-483.